

Optimal Design of UPFC Output Feed Back Controller for Power System Stability Enhancement by Hybrid PSO and GSA

Ahad Jahandideh shendi¹, Ali Ajami²

¹Department of electrical engineering, Sofian Branch, Islamic Azad University, Sofian, Iran.
Email: ajahandideh_msc@yahoo.com (Corresponding author)

²Department of Electrical Engineering, Azarbaijan Shahid Madani University, Tabriz, Iran
Email: ajami@azaruniv.edu

ABSTRACT

In this paper, the optimal design of supplementary controller parameters of a unified power flow controller (UPFC) for damping low-frequency oscillations in a weakly connected system is investigated. The individual design of the UPFC controller, using hybrid particle swarm optimization and gravitational search algorithm (PSOGSA) technique under 3 loading operating conditions, is discussed. The effectiveness of proposed controller on enhancing dynamic stability is tested through eigenvalue analysis and time domain simulation. Also nonlinear and electrical simulation results show the validity and effectiveness of the proposed control schemes over a wide range of loading conditions. It is also observed that the proposed UPFC-based damping stabilizers greatly enhance the power system transient stability. Also, simulation results of coordinated design of stabilizer based on δ_E and m_B is presented and discussed, the system performance analysis under different operating conditions show that the δ_E -based controller is superior to the m_B -based controller.

KEYWORDS: Power system dynamic stability, UPFC, PSOGSA

NOMENCLATURE

1 BT	boosting transformer	FACTS	flexible alternating current transmission systems
D	machine damping coefficient	PSS	power system stabilizer
DC	direct current	SMIB	single machine infinite bus
E'_q	internal voltage behind transient reactance	VSC	voltage source converter
E'_{fd}	equivalent excitation voltage	ΔV_{dc}	DC voltage deviation
K	proportional gain of the controller	GTO	gate turn off thyristor
K_A	regulator gain	m_E	excitation amplitude modulation ratio
M	machine inertia coefficient	m_B	boosting amplitude modulation ratio
P_e	active power	δ_B	boosting phase angle
P_m	mechanical input power	δ_E	excitation phase angle
PSO	particle swarm optimization	T_1	lead time constant of controller
GSA	gravitational search algorithm	T_2	lag time constant of controller
UPFC	unified power flow controller	T_3	lead time constant of controller
		T_4	lag time constant of controller
		T_A	regulator time constant
		T'_{do}	time constant of excitation circuit
		T_w	washout time constant

T_s	settling time of speed deviation
V_{ref}	reference voltage
W	rotor speed
δ	rotor angle

1. INTRODUCTION

The main priorities in a power system operation are its security and stability, so a control system should maintain its frequency and voltage at a fixed level against any kind of disturbance such as a sudden increase in load, a generator being out of circuit, or failure of a transmission line because of factors such as human faults, technical defects of equipments, natural disasters, etc. Due to the new legislation of electricity market, this situation creates doubled stress for beneficiaries [1-2]. Low frequency oscillations that are in the range of 0.2 to 3 Hz are created by the development of large power systems and their connection. These oscillations continue to exist in the system for a long time and if not well-damped, the amplitudes of these oscillations increase and bring about isolation and instability of the system [3-5]. Using a Power System Stabilizer (PSS) is technically and economically appropriate for damping oscillations and increasing the stability of power system. Therefore, various methods have been proposed for designing these stabilizers [6-8]. However, these stabilizers cause the power factor to become leading and therefore they have a major disadvantage which leads to loss of stability caused by large disturbances, particularly a three phase fault at the generator terminals [9]. In recent years, using Flexible Alternating Current Transmission Systems (FACTS) has been proposed as one of the effective methods for improving system controllability and limitations of power

transfer. By modeling bus voltage and phase shift between buses and reactance of transmission line, FACTS controllers can cause increment in power transfer in steady state. These controllers are added to a power system for controlling normal steady state but because of their rapid response, they can also be used for improving power system stability through damping the low frequency oscillation [1-4,10].

The unified power flow controller (UPFC) has various applications including loop flow control, power flow control, load sharing among parallel corridors, mitigation of system oscillations, and voltage (reactive power) regulation and enhancement of transient stability [11-12]. In order to carry out performance analysis and control synthesis of the UPFC, it is necessary to have its steady-state and dynamic models. A bi-source UPFC steady-state model including source impedances is suggested in [13]. Also a steady-state model, a small-signal linearized dynamic model, and a state-space large-signal model of a UPFC have been developed in [14], assuming that the power system is symmetrical and operates under 3-phase balanced conditions. In 1999, two UPFC models which have been linearized and incorporated into the Phillips-Heffron model were developed by Wang and were introduced in [15-16]. The UPFC damping controller design can be found in [1,3,17-20]. The supplementary controller can be applied to the series inverter through the modulation of the power reference signal or to the shunt inverter through the modulation index of the reference voltage signal. The particle swarm optimization (PSO) algorithm has been used in [1] and [3] to tune the optimum parameter settings of UPFC controllers for damping power system

oscillation. In [21], the real-coded genetic algorithm has been used for optimizing the damping controller parameters of the UPFC. Also, bacterial foraging has been used in [22] for the UPFC lead-lag type of controller parameter design.

In [23] the linear quadratic regulator method has been used by Lee and Yung for designing the state feedback gain of the static synchronous compensator (STATCOM) controller to increase the damping of a single-machine infinite-bus (SMIB) power system. In [22] the authors have used an adaptive improved PSO hybrid with simulated annealing to design a UPFC damping controller. In [19] a comprehensive comparison between the PSS, static VAR compensator, and STATCOM controllers for damping power system oscillations using the Hopf bifurcation theory, an “extended” eigenvalue analysis to study different controllers, their locations, and the use of various control signals for the effective damping of these oscillations has been presented. In [24] the authors have used of the imperialist competitive algorithm (ICA) technique for the optimal design of supplementary controller parameters of a unified power flow controller (UPFC) to damp low-frequency oscillations. In [25] Individual designs of the UPFC controller using adaptive improved particle swarm optimization hybrid with simulated annealing (AIPSO-SA) has been presented. In this paper, singular value decomposition (SVD) is used to select the control signal which is most suitable for damping the electromechanical (EM) mode oscillations. A single machine infinite bus (SMIB) power system equipped with a UPFC controller is used in this study. Also, the damping controllers design is formulated as an optimization problem to be solved using PSOGSA. This algorithm has been popular in academia and the industry mainly

because of its intuitiveness, ease of implementation, and the ability to effectively solve highly nonlinear optimization problems that are typical of complex engineering systems. It has been reported in the literature that PSOGSA is more efficient in terms of CPU time and offers higher precision with more consistent results [31]. The effectiveness of the proposed controller is demonstrated through eigenvalue analysis, nonlinear time simulation studies and some performance indices to damp low frequency oscillations under different operating conditions. Results evaluation show that the proposed PSOGSA-based tuned damping controller achieves good robust performance for a wide range of operating conditions.

2. PROPOSED ALGORITHMS

2.1. Particle swarm optimization (PSO)

PSO is an evolutionary computation technique which is proposed by Kennedy and Eberhart [26]. The PSO was inspired by the social behaviour of bird flocking. It uses a number of particles (candidate solutions) which fly around in the search space to find the best solution. Meanwhile, the particles all look at the best particle (best solution) in their paths. In other words, particles consider their own best solutions as well as the best solution found so far.

Each particle in PSO should consider the current position, the current velocity, the distance to $pbest$, and the distance to $gbest$ in order to modify its position. PSO was mathematically modelled as follows:

$$v_i^{t+1} = w \times v_i^t + c_1 \times rand(pbest_i - x_i^t) + c_2 \times rand(gbest_i - x_i^t) \quad (1)$$

$$x_i^{t+1} = x_i^t + v_i^{t+1} \quad (2)$$

where v_i^t is the velocity of particle i at

iteration t , w is a weighting function, c_j is an acceleration coefficient, $rand$ is a random number between 0 and 1, x_i^t is the current position of particle i at iteration t , $pbest_i$ is the $pbest$ of agent i at iteration t , and $gbest$ is the best solution so far.

The first part of (1), wv_i^t , provides exploration ability for PSO. The second and third parts, $c_1 \times rand \times (pbest_i - x_i^t)$ and $c_2 \times rand \times (gbest - x_i^t)$, represent private thinking and collaboration of particles respectively. The PSO starts by randomly placing the particles in a problem space. In each iteration, the velocities of particles are calculated using (1). After defining the velocities, the positions of particles can be calculated as (2). The process of changing particles' positions will continue until an end criterion is met.

2.2. Gravitational search algorithm (GSA)

In 2009, Rashedi et al. [27] proposed a new heuristic optimization algorithm called the Gravitational Search Algorithm (GSA) for finding the best solution in problem search spaces using physical rules. The basic physical theory from which GSA is inspired is Newton theory, which says: "Every particle in the universe attracts every other particle with a force that is directly proportional to the product of their masses and inversely proportional to the square of the distance between them". GSA can be considered as a collection of agents (candidate solutions) which have masses proportional to their value of fitness function. During generations all masses attract each other by the gravity forces between them. The heavier the mass, the bigger the attraction force. Therefore, the heaviest masses which are probably close to the global minimum attract the other masses in proportion to their distances.

According to [27-28], suppose there is a system with N agents. The position of each agent (masses) which is a candidate solution for the problem is defined as follows:

$$X_i = (x_i^1, \dots, x_i^d, \dots, x_i^n) \quad \text{for } i = 1, 2, \dots, N \quad (3)$$

where N is the dimension of the problem and x_i^d is the position of the i th agent in the d th dimension.

The algorithm starts by randomly placing all agents in a search space. During all epochs, the gravitational forces from agent j on agent i at a specific time t are defined as follows:

$$F_{ij}^d = G(t) \frac{M_{pi}(t) \times M_{aj}(t)}{R_{ij}(t) + \epsilon} (x_j^d(t) - x_i^d(t)) \quad (4)$$

Where M_{aj} is the active gravitational mass related to agent j , M_{pi} is the passive gravitational mass related to agent i , $G(t)$ is the gravitational constant at time t , ϵ is small constant, $R_{ij}(t)$ is the Euclidian distance between two agents i and j .

The gravitational constant G and the Euclidian distance between two agents i and j are calculated as follows:

$$G(t) = G_0 \times \exp(-\alpha \times \text{iter} / \text{maxiter}) \quad (5)$$

$$R_{ij}(t) = \|x_i(t), x_j(t)\|_2 \quad (6)$$

Where α is the descending coefficient, G_0 is the initial gravitational constant, iter is the current iteration, and maxiter is the maximum number of iterations.

In a problem space with the dimension d , the total force that acts on agent i is calculated by the following equation:

$$F_i^d(t) = \sum_{j=1, j \neq i}^N rand_j F_{ij}^d(t) \quad (7)$$

where $rand_j$ is a random number in the interval $[0, 1]$.

According to the law of motion, the acceleration of an agent is proportional to the resultant force and inverse of its mass,

so the accelerations of all agents are calculated as follows:

$$a_i^d(t) = \frac{F_i^d(t)}{M_{ii}(t)} \quad (8)$$

where d is the dimension of the problem, t is a specific time, and M_i is the mass of object i .

The velocity and position of agents are calculated as follows:

$$v_i^d(t+1) = rand_i \times v_i^d(t) + a_i^d(t) \quad (9)$$

$$x_i^d(t+1) = x_i^d(t) + v_i^d(t+1) \quad (10)$$

where d is the problem dimension and $rand_i$ is a random number in the interval $[0,1]$.

As can be inferred from (9) and (10), the current velocity of an agent is defined as a fraction of its last velocity ($0 \leq rand_i \leq 1$) added to its acceleration. Furthermore, the current position of an agent is equal to its last position added to its current velocity.

Agents' masses are defined using fitness evaluation. This means that an agent with the heaviest mass is the most efficient agent. According to the above equations, the heavier the agent, the higher the attraction force and the slower the movement. The higher attraction is based on the law of gravity (4), and the slower movement is because of the law of motion (8) [27].

The masses of all agents are updated using the following equations:

$$m_i(t) = \frac{fit_i(t) - worst(t)}{best(t) - worst(t)} \quad (11)$$

Where $fit_i(t)$ represents the fitness value of the agent i at time t , $best(t)$ is the strongest agent at time t , and $worst(t)$ is the weakest agent at time t .

$best(t)$ and $worst(t)$ for a minimization problem are calculated as follows:

$$best(t) = \min_{j \in \{1..N\}} fit_j(t) \quad (12)$$

$$worst(t) = \max_{j \in \{1..N\}} fit_j(t) \quad (13)$$

$best(t)$ and $worst(t)$ for a maximization problem are calculated as follows:

$$best(t) = \max_{j \in \{1..N\}} fit_j(t) \quad (14)$$

$$worst(t) = \min_{j \in \{1..N\}} fit_j(t) \quad (15)$$

The normalization of the calculated masses (11) is defined by the following equation:

$$M_i(t) = \frac{m_i(t)}{\sum_{j=1}^N m_j(t)} \quad (16)$$

In the GSA, at first all agents are initialized with random values. Each agent is a candidate solution. After initialization, the velocity and position of all agents will be defined using (9) and (10). Meanwhile, other parameters such as the gravitational constant and masses will be calculated by (5) and (11). Finally, the GSA will be stopped by meeting an end criterion. The steps of GSA are represented in Fig. 1.

In all population-based algorithms which have social behaviour like PSO and GSA, two intrinsic characteristics should be considered: the ability of the algorithm to explore whole parts of search spaces and its ability to exploit the best solution. Searching through the whole problem space is called exploration whereas converging to the best solution near a good solution is called exploitation. A population-based algorithm should have these two vital characteristics to guarantee finding the best solution. In PSO, the exploration ability has been implemented using Pbest and the exploitation ability has been implemented using Gbest. In GSA, by choosing proper values for the random parameters (G_0 and α), the exploration can be guaranteed and slow movement of heavier agents can guarantee the exploitation ability [27, 29]. Rashedi et al.[27] provided a comparative study between GSA and some well-known heuristic optimization algorithms like PSO.

The results proved that GSA has merit in the field of optimization. However, GSA suffers from slow searching speed in the last iterations [30]. In this paper a hybrid of this algorithm with PSO, called PSO-GSA, is proposed in order to improve this weakness.

2.3. The hybrid PSO-GSA algorithm

The basic idea of PSO-GSA is to combine the ability for social thinking (*gbest*) in PSO with the local search capability of GSA. In order to combine these algorithms, (17) is proposed as follows:

$$v_i(t+1) = w \times v_i(t) + c'_1 \times rand \times ac_i(t) + c'_2 \times rand \times (gbest_i - x'_i) \quad (17)$$

where $V_i(t)$ is the velocity of agent i at iteration t ; c'_j is an acceleration coefficient, w is a weighting function, $rand$ is a random number between 0 and 1, $ac_i(t)$ is the acceleration of agent i at iteration t , and $gbest$ is the best solution so far.

In each iteration, the positions of agents are updated as follows:

$$x_i(t+1) = x_i(t) + v_i(t+1) \quad (18)$$

In PSO-GSA, at first, all agents are randomly initialized. Each agent is considered as a candidate solution. After initialization, the gravitational force, gravitational constant, and resultant forces among agents are calculated using (4), (5) and (7) respectively. After that, the accelerations of particles are defined as (8). In each iteration, the best solution so far

should be updated. After calculating the accelerations and updating the best solution so far, the velocities of all agents can be calculated using (17). Finally, the positions of agents are updated by (18). The process of updating velocities and positions will be stopped by meeting an end criterion. The steps of PSO-GSA are represented in Fig. 2. To see how PSO-GSA is efficient, the following remarks are noted:

- In PSO-GSA, the quality of solutions (fitness) is considered in the updating procedure.
- The agents near good solutions try to attract the other agents which are exploring different parts of the search space.
- When all agents are near a good solution, they move very slowly. In this case, *gbest* helps them to exploit the global best.
- PSO-GSA uses a memory (*gbest*) to save the best solution found so far, so it is accessible at any time.
- Each agent can observe the best solution (*gbest*) and tend toward it.
- By adjusting c'_1 and c'_2 , the abilities of global searching and local searching can be balanced

The above-mentioned remarks make PSO-GSA powerful enough to solve a wide range of optimization problems [31].

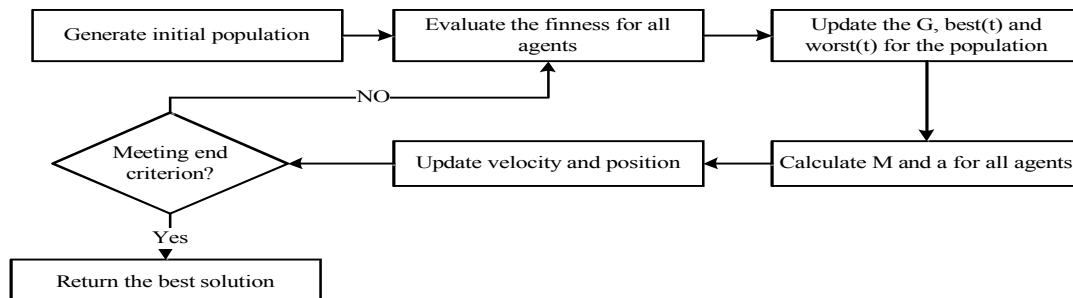


Fig. 1. General steps of the gravitational search algorithm [27] .

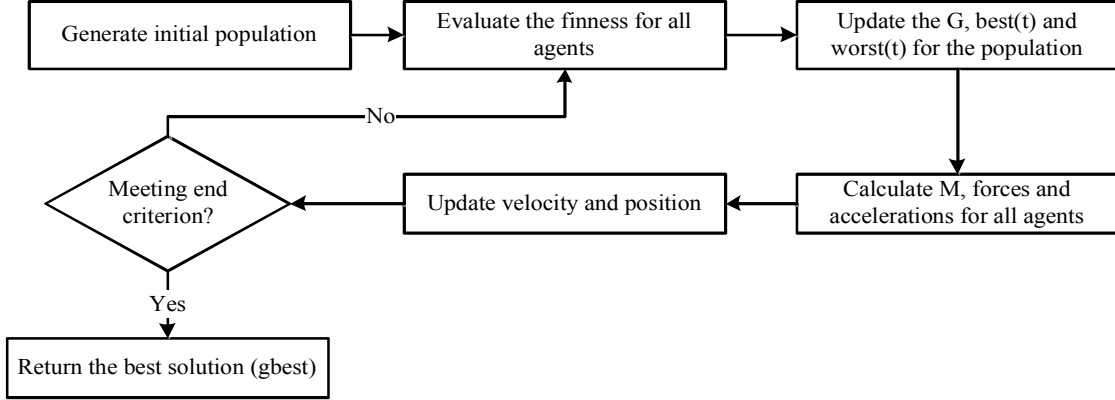


Fig. 2. Steps of PSO-GSA [31] .

3. DESCRIPTION OF CASE STUDY SYSTEM

Fig3 shows the test power system with a UPFC. In this paper, the test power system is an SMIB with 2 parallel lines. It can be seen from Fig3 that the UPFC has 4 input control signals. These control signals are m_E , m_B , δ_E , and δ_B , where, m_E is the excitation amplitude modulation ratio, m_B is the boosting amplitude modulation ratio, δ_E is the excitation phase angle and δ_B is the boosting phase angle. The parameters of the test power system are given in the Appendix.

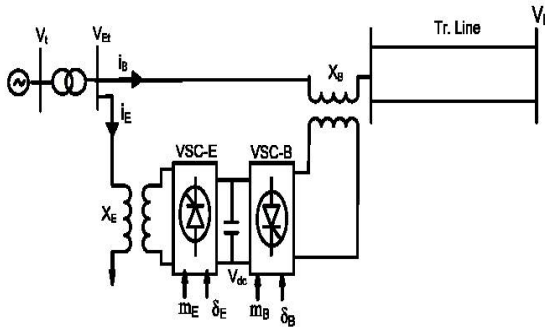


Fig. 3. SMIB power system equipped with UPFC.

3.1. System nonlinear model with UPFC

In this section, to study the effect of the UPFC in the small-signal stability improvement of a power system, a dynamic

model of a UPFC is presented. While neglecting the resistance and transients of the excitation (ET) and boosting (BT) transformers in Fig 3, the UPFC model in the dq reference frame can be obtained as [1,3,13,15].

$$\begin{bmatrix} v_{Ed} \\ v_{Eq} \end{bmatrix} = \begin{bmatrix} 0 & -x_E \\ x_E & 0 \end{bmatrix} \begin{bmatrix} i_{Ed} \\ i_{Eq} \end{bmatrix} + \begin{bmatrix} \frac{m_E \cos \delta_E v_{dc}}{2} \\ \frac{m_E \sin \delta_E v_{dc}}{2} \end{bmatrix} \quad (19)$$

$$\begin{bmatrix} v_{Bd} \\ v_{Bq} \end{bmatrix} = \begin{bmatrix} 0 & -x_B \\ x_B & 0 \end{bmatrix} \begin{bmatrix} i_{Bd} \\ i_{Bq} \end{bmatrix} + \begin{bmatrix} \frac{m_B \cos \delta_B v_{dc}}{2} \\ \frac{m_B \sin \delta_B v_{dc}}{2} \end{bmatrix} \quad (20)$$

$$v_{dc}^* = \frac{3m_E}{4C_{dc}} \begin{bmatrix} \cos \delta_E & \sin \delta_E \end{bmatrix} \begin{bmatrix} i_{Ed} \\ i_{Eq} \end{bmatrix} + \frac{3m_B}{4C_{dc}} \begin{bmatrix} \cos \delta_B & \sin \delta_B \end{bmatrix} \begin{bmatrix} i_{Bd} \\ i_{Bq} \end{bmatrix} \quad (21)$$

In the above equations, v_{Et} , i_E , v_{Bt} , and i_B represent the voltage and current of the excitation and boosting transformers, respectively, and v_{dc} and C_{dc} show the DC link voltage and DC link capacitance, respectively. When considering the circuit equations of Fig.3 and some simplifications, the currents of the excitation and boosting transformers and line 2 in the dq reference frame can be written as:

$$i_{TLd} = \frac{1}{x_T} \left(x_E i_{Ed} + \frac{m_E \sin \delta_E v_{dc}}{2} - v_b \cos \delta \right) \quad (22)$$

$$i_{TLq} = \frac{1}{x_T} \left(x_E i_{Eq} - \frac{m_E \cos \delta_E v_{dc}}{2} + v_b \sin \delta \right) \quad (23)$$

$$i_{Ed} = \frac{x_{BB}}{x_{d2}} E'_q + x_{d7} \frac{m_B \sin \delta_B v_{dc}}{2} + x_{d5} v_b \cos \delta + x_{d6} \frac{m_E \sin \delta_E v_{dc}}{2} \quad (24)$$

$$i_{Eq} = x_{q7} \frac{m_B \cos \delta_B v_{dc}}{2} + x_{q5} v_b \sin \delta + x_{q6} \frac{m_E \cos \delta_E v_{dc}}{2} \quad (25)$$

$$i_{Bd} = \frac{x_E}{x_{d2}} E'_q - \frac{x_{d1}}{x_{d2}} \frac{m_B \sin \delta_B v_{dc}}{2} + x_{d3} v_b \cos \delta + x_{d4} \frac{m_E \sin \delta_E v_{dc}}{2} \quad (26)$$

$$i_{Bq} = \frac{x_{q1}}{x_{q2}} \frac{m_B \cos \delta_B v_{dc}}{2} + x_{q3} v_b \sin \delta + x_{q4} \frac{m_E \cos \delta_E v_{dc}}{2} \quad (27)$$

where x_E and x_B represent the leakage reactance of the ET and BT, respectively, and the reactances x_{qE} , x_{dE} , x_{BB} , x_{d1} – x_{d7} , and x_{q1} – x_{q7} are given in [32].

The conventional nonlinear dynamic equations of the generator shown in the SMIB test system in Fig.3 are:

$$\dot{\delta} = \omega_b (\omega - 1) \quad (28)$$

$$\dot{\omega} = \frac{1}{M} (P_m - P_e - D\Delta\omega) \quad (29)$$

$$\dot{E}'_q = \frac{1}{T'_{do}} (E_{fd} - (x_d - x'_d) i_d - E'_q) \quad (30)$$

$$\dot{E}_{fd} = -\frac{1}{T_A} E_{fd} + \frac{K_A}{T_A} (V_{ref} - v + u_{pss}) \quad (31)$$

where

$$P_e = v_d i_d + v_q i_q, \quad v_d = x_q i_q, \quad v_q = E'_q - x'_d i_d$$

$$i_d = i_{Ed} + i_{Bd} + i_{TLd}, \quad i_q = i_{Eq} + i_{Bq} + i_{TLq},$$

$$v = (v_d^2 + v_q^2)^{1/2}$$

Above, P_m is the mechanical input power of the generator; P_e is the electrical output power of the generator; M and D are the inertia constant and damping coefficient;

ω_b is the synchronous speed of the generator; δ and ω are the rotor angle and speed; E'_q , E_{fd} , and v are the generator internal voltage, field voltage, and terminal voltage, respectively; T'_{do} is the open-circuit field time constant; x_d , x'_d , and x_q are the generator reactance in the d-axis, d-axis transient reactance, and q-axis reactance, respectively; K_A and T_A are the gain and time constant of the generator exciter, respectively; V_{ref} is the AC bus reference voltage; and u_{pss} is the control signal of the PSS.

3.2. Linearized model of the power system
In this paper, in order to perform a stability evaluation, eigenvalue analysis is used. For this purpose and to obtain the eigenvalues of the system, the nonlinear dynamic equations of the test power system must be linearized around an operating point condition. Eqs. (32) through (36) show the linearized model of the test power system from Fig.3.

$$\Delta \dot{\delta} = \omega_b \Delta \omega \quad (32)$$

$$\Delta \dot{\omega} = (-\Delta P_e - D \Delta \omega) / M \quad (33)$$

$$\Delta \dot{E}'_q = (-\Delta E_q + \Delta E_{fd} + (x_d - x'_d) \Delta i_d) / T'_{do} \quad (34)$$

$$\Delta \dot{E}_{fd} = \frac{1}{T_A} (-\Delta E_{fd} + K_A (\Delta V_{ref} - \Delta V_t + \Delta u_{pss})) \quad (35)$$

$$\Delta \dot{V}_{dc} = K_7 \Delta \delta + K_8 \Delta E'_q - K_9 \Delta V_{dc} + K_{ce} \Delta m + K_{c\delta e} \Delta \delta_E + K_{cb} \Delta m_B + K_{c\delta b} \Delta \delta_B \quad (36)$$

In the state-space representation, the power system can be modeled as:

$$\dot{X} = Ax + Bu \quad (37)$$

where the state vector x , control vector u , state matrix A , and input matrix B are:

$$x = [\Delta \delta \quad \Delta \omega \quad \Delta E'_q \quad \Delta E_{fd} \quad \Delta v_{dc}]^T$$

$$u = [\Delta u_{pss} \quad \Delta m_E \quad \Delta \delta_E \quad \Delta m_B \quad \Delta \delta_B]^T$$

$$A = \begin{bmatrix} 0 & w_b & 0 & 0 & 0 \\ -\frac{K_1}{M} & 0 & -\frac{K_2}{M} & 0 & -\frac{K_{pd}}{M} \\ -\frac{K_4}{T'_{do}} & 0 & \frac{K_3}{T'_{do}} & \frac{1}{T'_{do}} & -\frac{K_{qd}}{T'_{do}} \\ -\frac{K_A K_5}{T_A} & 0 & -\frac{K_A K_6}{T_A} & -\frac{1}{T_A} & -\frac{K_A K_{vd}}{T_A} \\ K_7 & 0 & K_8 & 0 & -K_9 \end{bmatrix},$$

$$B = \begin{bmatrix} 0 & 0 & 0 & 0 & 0 \\ 0 & -\frac{K_{pe}}{M} & -\frac{K_{p\delta e}}{M} & -\frac{K_{pb}}{M} & -\frac{K_{p\delta b}}{M} \\ 0 & -\frac{K_{qe}}{T'_{do}} & -\frac{K_{q\delta e}}{T'_{do}} & -\frac{K_{qb}}{T'_{do}} & -\frac{K_{q\delta b}}{T'_{do}} \\ \frac{K_A}{T_A} & -\frac{K_A K_{ve}}{T_A} & -\frac{K_A K_{v\delta e}}{T_A} & -\frac{K_A K_{vb}}{T_A} & -\frac{K_A K_{v\delta b}}{T_A} \\ 0 & K_{ce} & K_{c\delta e} & K_{cb} & K_{c\delta b} \end{bmatrix}$$

The linearized dynamic model of the state-space representation is shown in Fig 4.

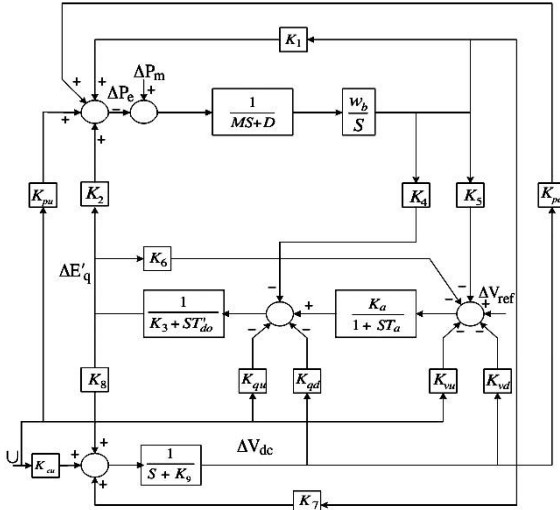


Fig. 4. Modified Heffron–Phillips transfer function model.

3.3. UPFC-based damping controller

The damping controller is designed to produce an electrical torque, according to the phase compensation method, in phase with the speed deviation. In order to produce the damping torque, four control parameters of the UPFC (m_E , δ_E , m_B , and δ_B) can be modulated.

In this paper, δ_E and m_B are modulated in order to damping controller design. The speed deviation $\Delta\omega$ is chosen as the input to the damping controller. Fig.5 shows the structure of the UPFC-based damping controller [1,3,5]. This controller may be considered as a lead-lag compensator. However, an electrical torque in phase with the speed deviation is to be produced to improve the damping of the power system oscillations. It consists of a gain block, a signal-washout block, and lead-lag compensator. The parameters of the damping controller are obtained using the PSO-GSA technique.

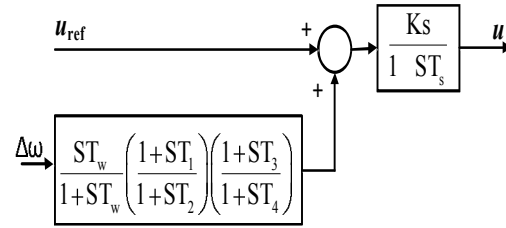


Fig 5. UPFC with a lead-lag controller.

4. UPFC CONTROLLER DESIGN USING THE PSO-GSA

In the proposed method, the UPFC controller parameters must be tuned optimally to improve overall system dynamic stability in a robust way. This study employs the PSO-GSA to improve optimization synthesis and find the global optimum value of the fitness function in order to acquire an optimal combination. In this study, the PSO-GSA module works offline. In other words, the parameters of the UPFC damping controller are tuned for different loading conditions and system parameter uncertainties based on Table 1, and then the obtained optimal parameters of the damping controller are applied to the time-domain simulation.

Table 1. Loading condition

Operating conditions	P (pu)	Q (pu)	X_L (pu)
Normal	0.8	0.114	0.3
Light	0.2	0.01	0.3
Heavy	1.2	0.4	0.3
Case 4	the 30% increase of line reactance XL at nominal loading condition		
Case 5	the 30% increase of line reactance XL at heavy loading condition		

For our optimization problem, an integral time absolute error of the speed deviations is taken as the objective function J , expressed as:

$$J = \int_0^{t_1} |e(t)| t dt \quad (38)$$

Where, ‘e’ is the error signal ($\Delta\omega$) and t_1 is the time range of simulation.

The optimization problem design can be formulated as the constrained problem shown below, where the constraints are the

controller parameters bounds.

Minimize J

Subject to

$$K_{\min} \leq K \leq K_{\max}$$

$$T_{1\min} \leq T_1 \leq T_{1\max}$$

$$T_{2\min} \leq T_2 \leq T_{2\max}$$

$$T_{3\min} \leq T_3 \leq T_{3\max}$$

$$T_{4\min} \leq T_4 \leq T_{4\max}$$

(39)

Typical ranges of the optimized parameters are [0, 100] for K and [0.01, 1] for T_1 , T_2 , T_3 , and T_4 . The mentioned approach employs the PSOGSA to solve this optimization problem and searches for an optimal or near-optimal set of controller parameters. It should be noted that PSOGSA algorithm is run several times and then optimal set of output feedback gains for the UPFC controllers is selected. The final values of the optimized parameters are given in Table 2. Fig.6 shows the illustration of cost versus iteration for both the δ_E -and m_B -based controllers using the PSO, GSA and PSOGSA techniques.

Table 2.The optimal settings of the individual controller

controller parametes	m_B			δ_E		
	PSO	GSA	PSOGSA	PSO	GSA	PSOGSA
K	73.8019	62.6673	81.3002	84.3309	76.6433	83.9329
T_1	0.7008	0.3887	0.4363	0.9447	0.9347	0.8017
T_2	0.4822	0.7517	0.6890	0.1334	0.1201	0.3188
T_3	0.9978	0.1944	0.9257	0.3332	0.5180	0.8281
T_4	0.0669	0.0603	0.1119	0.0818	0.2554	0.0171

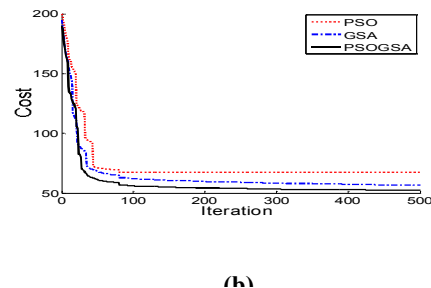
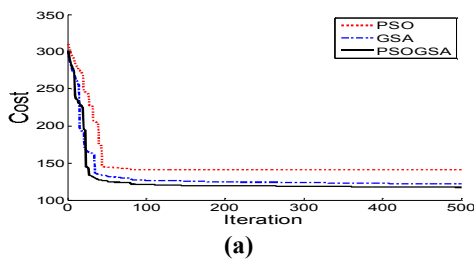


Figure.6. The convergence for objective function minimization using PSO, GSA and PSOGSA techniques :

(a): m_B -based controller, (b): δ_E -based controller.

5. SIMULATION RESULTS

In order to demonstrate the effectiveness and robustness of the proposed controller, against severe turbulence and the damping of oscillations caused by it, power system using the proposed model, is simulated in MATLAB software. To make sure that the obtained results are reliable, this simulation is evaluated with eigenvalue analysis method and time domain nonlinear simulation, which is shown as follows.

5.1. Eigenvalue Analysis

The electromechanical modes and the damping ratios obtained for all operating conditions both with and without proposed controllers in the system are given in Table. 3 and 4. Given a complex eigenvalue, [5]:

$$\xi = -\frac{\sigma}{\sqrt{\sigma^2 + \mu^2}} \quad (40)$$

When UPFC is not installed, it can be seen that some of the modes are poorly damped and in some cases, are unstable (highlighted in Table 3 and 4).

Table 3. Eigenvalues and damping ratios of electromechanical modes with and without δ_E controller

Controller Loding Condition	without controller	PSO controller	GSA controller	PSOGSA Controller
Nominal loading condition Eigenvalue (damping ratio)	0.0663 ± 8.6962i, (-0.076) -0.4778, -0.0742 -20.0678	-8.0014 ± 7.0712i, (0.749) -0.5577 ± 0.8434i, (0.551) -0.5531 ± 0.1742i, (0.953) -0.2529, -20.1713	-9.8349 ± 1.2659i, (0.991) -0.5524 ± 0.1692i, (0.956) -0.4548, -0.4842 -0.8712, -20.3216	-0.5326 ± 0.1968i, (0.938) -0.4548 ± 0.3019i, (0.833) -1.0200, -5.0062 -18.7853, -21.8784
Light loading condition Eigenvalue (damping ratio)	0.0223 ± 7.961i, (-0.028) -0.371, -0.0426 -20.438	-8.0160 ± 7.0143i, (0.752) -0.5017 ± 0.7019i, (0.581) -0.7845 ± 0.2474i, (0.953) -0.2520, -20.987	-9.3441 ± 1.6052i, (0.985) -0.4352 ± 0.6981i, (0.529) -0.4041, -0.4340 -0.7019, -18.2169	-0.4532 ± 0.1696i, (0.936) -0.4037 ± 0.2369i, (0.862) -0.9243, -5.0316 -18.8054, -20.8998
Heavy loading condition Eigenvalue (damping ratio)	0.0461 ± 8.1912i, (-0.056) -0.4008, -0.7432 -18.673	-9.1984 ± 8.7923i, (0.722) -0.6001 ± 0.7143i, (0.643) -0.5511 ± 0.1318i, (0.972) -0.2682, -18.7139	-9.3499 ± 1.2591i, (0.991) -0.5929 ± 0.1889i, (0.952) -0.4941, -0.4099 -0.8919, -20.2872	-0.5022 ± 0.1916i, (0.934) -0.4214 ± 0.1889i, (0.912) -1.2316, -5.0426 -16.1354, -21.9735
Case 4 loading condition Eigenvalue (damping ratio)	0.0432 ± 8.1275i, (-0.053) -0.3986, -0.0646 -19.2165	-8.3217 ± 7.1653i, (0.757) -0.5097 ± 0.8074i, (0.533) -0.5963 ± 0.1701i, (0.961) -0.3189, -20.015	-9.9219 ± 1.6215i, (0.986) -0.5023 ± 0.1312i, (0.967) -0.3985, -0.4056 -0.8022, -19.4379	-0.6013 ± 0.1857i, (0.955) -0.4843 ± 0.3956i, (0.774) -1.1120, -4.1248 -18.4223, -21.0549
Case 5 loading condition Eigenvalue (damping ratio)	0.0334 ± 7.1289i, (-0.046) -0.3991, -0.0401 -19.428	-8.2160 ± 7.5213i, (0.737) -0.4986 ± 0.6973i, (0.581) -0.7218 ± 0.2189i, (0.956) -0.2521, -20.917	-9.1481 ± 1.2945i, (0.990) -0.4182 ± 0.6019i, (0.570) -0.4312, -0.4951 -0.7184, -18.9321	-0.4012 ± 0.1121i, (0.963) -0.6246 ± 0.3421i, (0.877) -0.9931, -5.1136 -18.9934, -20.3328

Table 4. Eigenvalues and damping ratios of electromechanical modes with and without m_B controller

Controller Loding Condition	without controller	PSO controller	GSA controller	PSOGSA Controller
Nominal loading condition Eigenvalue (damping ratio)	0.0663 ± 8.6962i, (-0.076) -0.4778, -0.0742 -20.0678	-5.9119 ± 5.4726i, (0.733) -0.5309 ± 0.0739i, (0.990) -0.3493, -0.4386 -0.1771, -19.1459	-6.5215 ± 4.3600i, (0.831) -0.5764 ± 0.0574i, (0.995) -0.3792, -0.4188 -0.1766, -19.1676	-7.6405 ± 3.2901i, (0.918) -0.8275 ± 0.2550i, (0.955) -0.5022, -0.1818 -0.4270, -20.2031
Light loading condition Eigenvalue (damping ratio)	0.0223 ± 7.961i, (-0.028) -0.371, -0.0426 -20.438	-5.1756 ± 5.2091i, (0.704) -0.5311 ± 0.0709i, (0.991) -0.4922, -0.4021 -0.1643, -18.5076	-6.01327 ± 4.1384i, (0.823) -0.5604 ± 0.0511i, (0.995) -0.3087, -0.5859 -0.7381, -18.3279	-6.1465 ± 3.9211i, (0.843) -0.8001 ± 0.2364i, (0.959) -0.6130, -0.1076 -0.4021, -20.6643
Heavy loading condition Eigenvalue	0.0461 ± 8.1912i, (-0.056) -0.4008, -0.7432 -18.673	-6.1543 ± 4.7166i, (0.793) -0.5499 ± 0.1731i, (0.953) -0.3043, -0.4918	-8.4338 ± 5.6871i, (0.829) -0.4326 ± 0.1215i, (0.962) -0.3711, -0.4033	-8.6493 ± 3.9543i, (0.909) -0.7587 ± 0.3212i, (0.920) -0.5943, -0.8532

(damping ratio)		-0.7915, -16.5348	-0.2312, -16.8351	-0.2115, -18.6732
Case 4 loading condition	0.0432 ± 8.1275i, (-0.053)	-5.0219 ± 5.7112i, (0.660)	-6.3321 ± 4.1976i, (0.833)	-8.7890 ± 4.8719i, (0.874)
Eigenvalue (damping ratio)	-0.3986, -0.0646	-0.3319 ± 0.0661i, (0.980)	-0.5098 ± 0.2214i, (0.917)	-0.7765 ± 0.4432i, (0.868)
	-19.2165	-0.4243, -0.4898	-0.4436, -0.4567	-0.6783, -0.2134
		-0.2231, -19.3249	-0.3215, -19.1032	-0.4991, -20.5529
Case 5 loading condition	0.0334 ± 7.1289i, (-0.046)	-5.4551 ± 5.1181i, (0.729)	-7.8864 ± 4.9974i, (0.844)	-7.5541 ± 4.5321i, (0.857)
Eigenvalue (damping ratio)	-0.3991, -0.0401	-0.6043 ± 0.1129i, (0.982)	-0.5032 ± 0.1123i, (0.975)	-0.8861 ± 0.3245i, (0.939)
	-19.428	-0.5532, -0.4912	-0.3332, -0.5987	-0.6124, -0.1747
		-0.4321, -18.0233	-0.7765, -18.7895	-0.4428, -20.3323

5.2. Nonlinear time-domain simulation

The single-machine infinite-bus system shown in Fig. 3 is considered for nonlinear simulation studies. 6-cycle 3-phase fault at $t = 1$ s, on the infinite bus has occurred, at all loading conditions given in Table 1, to study the performance of the proposed controller. The speed deviation and

electrical power deviation based on the δ_E and m_B controller in three different loading conditions are shown in Figs. 7-16. It can be seen that the PSO GSA based UPFC controller tuned using the objective function achieves good robust performance and provides superior damping.

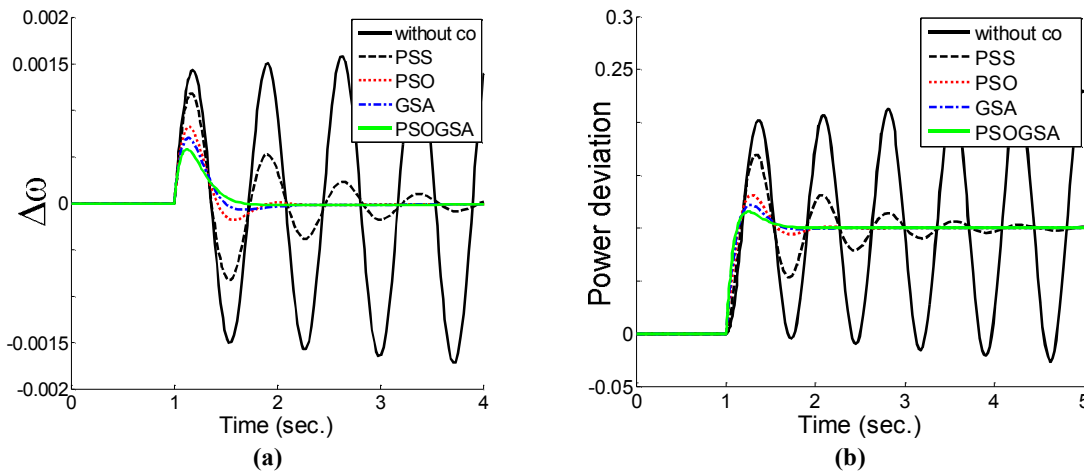


Fig. 7. Dynamic responses for (a) $\Delta\omega$, (b) ΔP with and without m_B controller at Normal loading condition

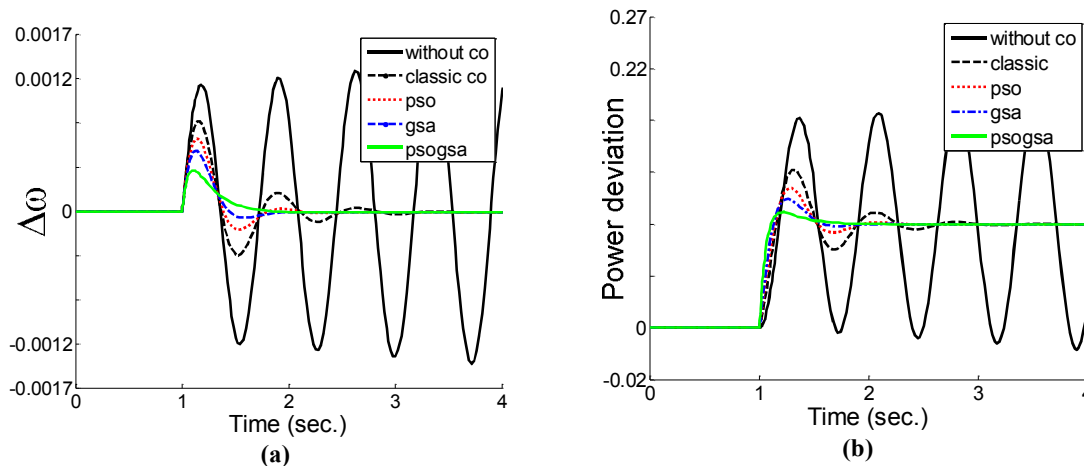


Fig. 8. Dynamic responses for (a) $\Delta\omega$, (b) ΔP with and without m_B controller at light loading condition

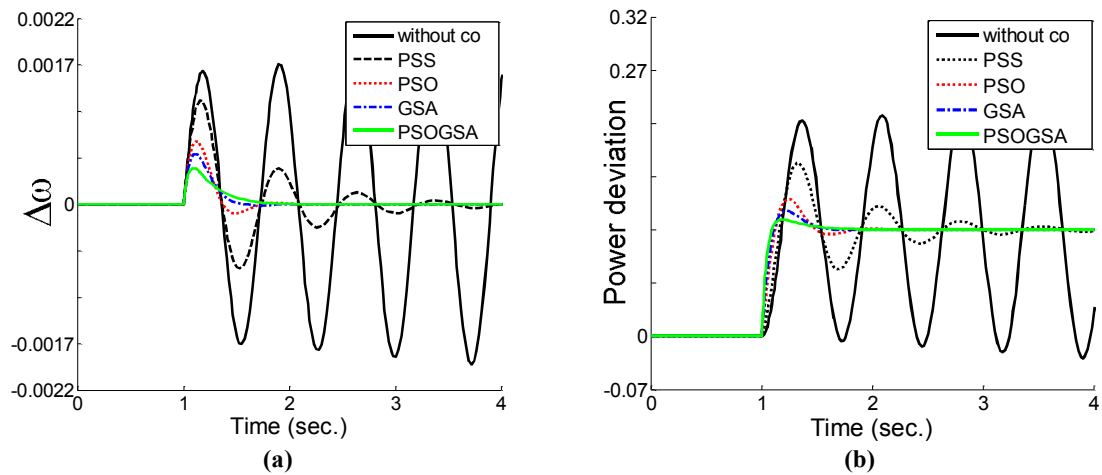


Fig. 9. Dynamic responses for (a) $\Delta\omega$, (b) ΔP with and without m_B controller at heavy loading condition

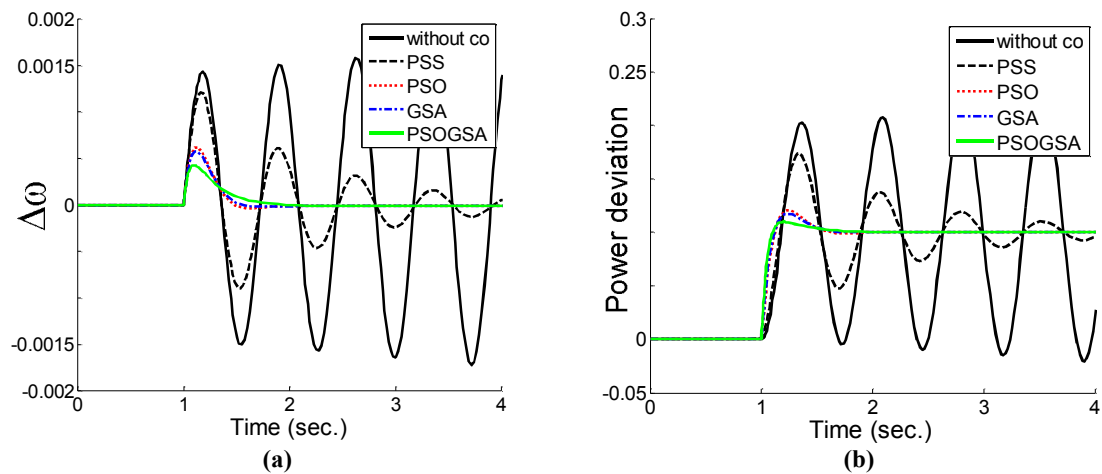


Fig. 10. Dynamic responses for (a) $\Delta\omega$, (b) ΔP with and without m_B controller at case 4 loading condition

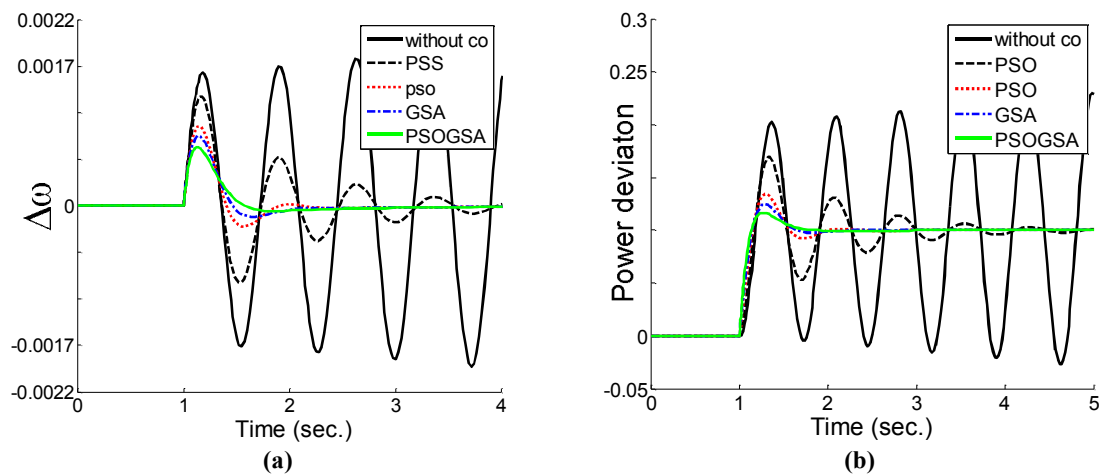


Fig. 11. Dynamic responses for (a) $\Delta\omega$, (b) ΔP with and without m_B controller at case 5 loading condition

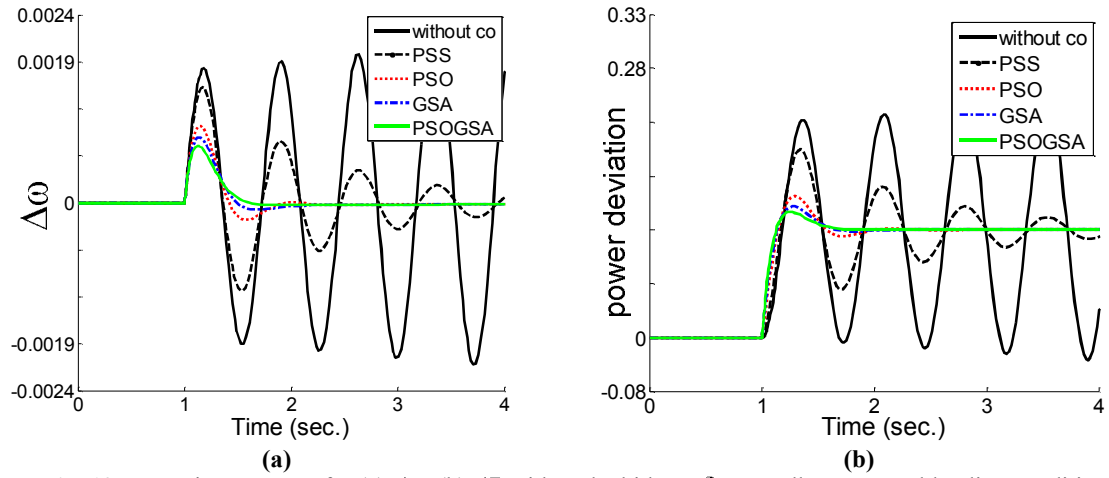


Fig. 12. Dynamic responses for (a) $\Delta\omega$, (b) ΔP with and with out δ_E controller at normal loading condition

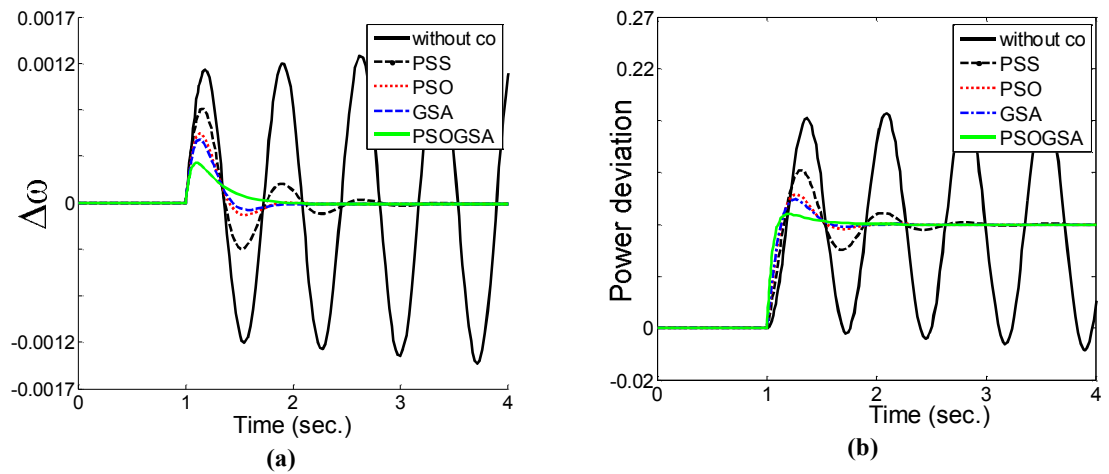


Fig. 13. Dynamic responses for (a) $\Delta\omega$, (b) ΔP with and with out δ_E controller at light loading condition

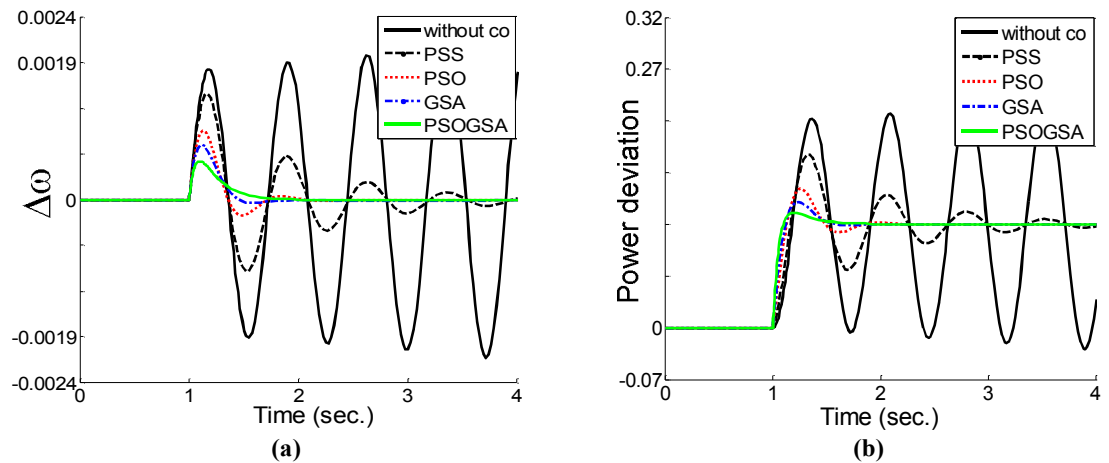


Fig. 14. Dynamic responses for (a) $\Delta\omega$, (b) ΔP with and with out δ_E controller at heavy loading condition

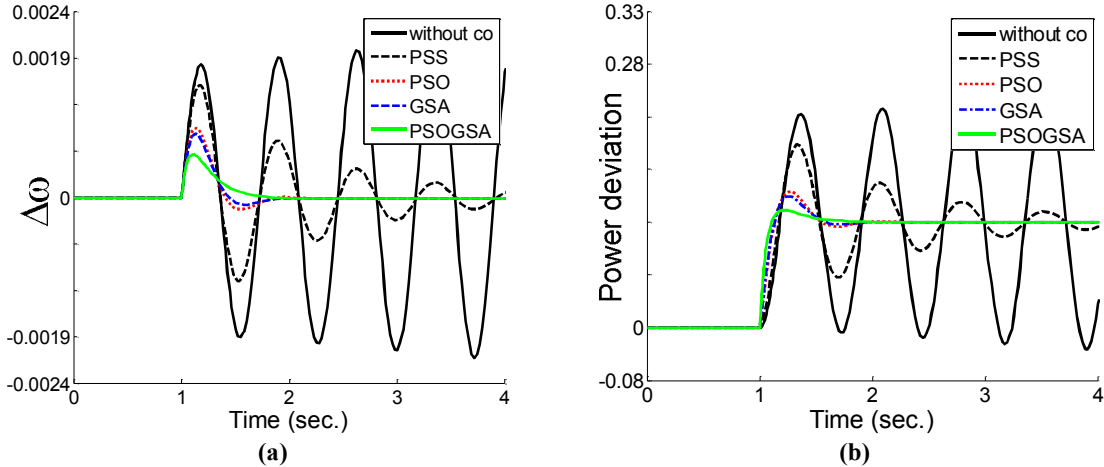


Fig. 15. Dynamic responses for (a) $\Delta\omega$, (b) ΔP with and with out δ_E controller at case4 loading condition

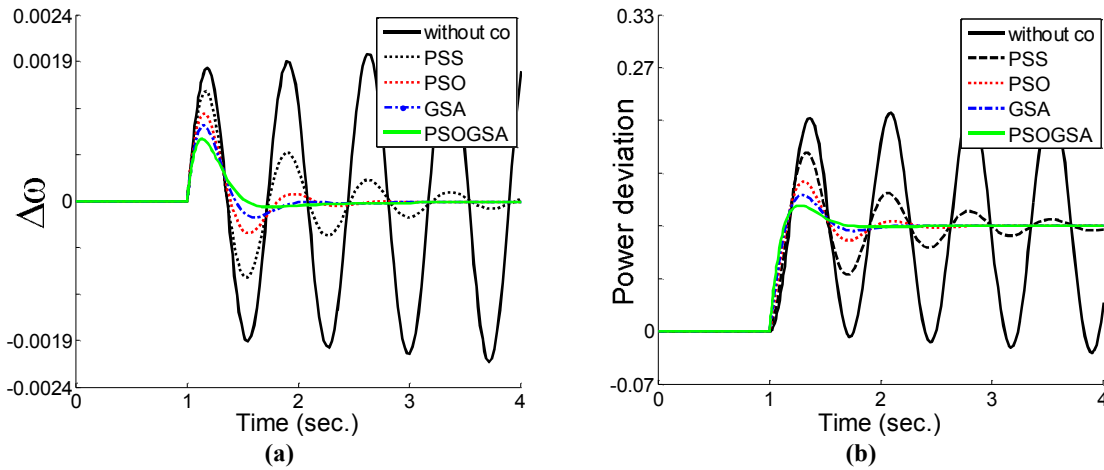


Fig. 16. Dynamic responses for (a) $\Delta\omega$, (b) ΔP with and with out δ_E controller at case5 loading condition

6. CONCLUSION

In this paper, low-frequency oscillation damping using a UPFC controller was investigated. The stabilizer was tuned to simultaneously shift the undamped electromechanical modes of the machine to the left side of the s-plane. An objective problem comprising the damping ratio of the undamped electromechanical modes was formulated to optimize the controller parameters. The design problem of the

controller was converted into an optimization problem, The PSOGSA optimization technique has been proposed to design the UPFC controllers individually and δ_E , m_B coordinately. PSO, GSA and PSOGSA have been utilized to search for the optimal controller parameter settings that optimize a damping ratio based objective function. The effectiveness of the proposed UPFC controller for damping low-frequency oscillations of a power

system were demonstrated by a weakly connected example power system subjected to a disturbance. The eigenvalue analysis and time-domain simulation results showed the effectiveness of the proposed controller in damping low-frequency oscillations, also the system performance analysis under different operating conditions show that the δ_E -based controller is superior to the m_B based controller.

APPENDIX

The nominal parameters and operating condition of the system are listed in table 5.

Table 5. System parameters

Generator	M = 8 MJ/MVA $T'_{do}=5.044$ $X_d=1$ pu	$X_q=0.6$ pu $X'_d=0.3$ pu D=4
Excitation system	$K_A=80$	$T_A=0.05$ s
Transformers	$X_T=0.1$ pu $X_B=0.1$ pu	$X_E=0.1$ pu
Transmission line	$X_L=1$ pu	
Operating condition	P = 0.8 pu	Vb=1.0 pu
	$V_t=1.0$ pu	
DC link parameter	$V_{DC}=2$ pu	$C_{DC}=1$ pu
UPFC parameter	$m_B=0.08$	$\delta_B=78.21$
	$\delta_E=85.35$	$m_E=0.4$
	$K_s=1$	$T_s=0.05$

REFERENCES

- [1] A.T. Al-Awami, Y. L. Abdel-Magid, M. A. Abido, "A particle-swarm-based approach of power system stability enhancement with unified power flow controller", *International Journal of Electric Power and Energy Systems*, vol. 29, no. 3, pp. 251 – 259, 2007
- [2] P. M. Anderson, A. A. Fouad, "Power System Control and Stability", Ames, IA: Iowa State University Press, 1977.
- [3] H. Shayeghi, H. A. Shayanfar, S. Jalilzadeh, A. Safari, "A PSO based unified power flow controller for damping of power system oscillations", *Energy Conversion and Management*, vol. 50, no.10, pp. 2583-2592, 2009.
- [4] H. Shayeghi, H. A. Shayanfar, S. Jalilzadeh, A. Safari, "Design of output feedback UPFC controller for damping of electromechanical oscillations using PSO", *Energy Conversion and Management*, vol. 50, no.10, pp. 2554-2561, 2009.
- [5] Ali Ajami and Mehdi Armaghan, "Application of multi-Objective PSO algorithm for power system stability enhancement by means of SSSC", *International Journal of Computer and Electrical Engineering*, vol. 2, no. 5, pp. 1793-8163, 2010
- [6] M. A. Abido, "Robust design of multimachine power system stabilizers using simulated annealing", *IEEE Trans. Energy Conversion*, vol. 15, no. 3, pp. 297-304, 2000.
- [7] Chun liu, Ryuichi Yokoyama, Kaoru Koyanagi, Kwang Y. Lee, "PSS design for damping of inter-area power oscillations by coherency-based equivalent model", *International Journal of Electrical Power and Energy Systems*, vol. 26, no. 7, pp. 535-544, 2004.
- [8] P. Kundur, M. Klein, G.J. Rogers, M.S. Zywno, "Application of power system stabilizers for enhancement of overall system stability", *IEEE Trans. on Power System*, vol. 4, no. 2, pp. 614-626, 1989.
- [9] A. J. F. Keri, X. Lombard, A. A. Edris, "Unified power flow controller: modeling and analysis", *IEEE Trans. on Power Systems*, vol. 14, no. 2, pp. 648-654, 1999.
- [10] M. R. Banaei, A. Kami, "Interline power flow controller (IPFC) based damping recurrent neural network controllers for enhancing stability", *Energy Conversion and Management*, vol. 52, no.7, pp. 2629-2636, 2011.
- [11] L. Gyugyi, C.D. Schauder, S. L. Williams, T. R. Rietman, D. R. Torgerson, A. Edris, "The unified power flow controller: a new approach to power transmission control", *IEEE Trans. on Power Delivery*, vol. 10, no. 2, pp.1085-1097, 1995.
- [12] L. Gyugyi, "A unified power flow control concept for flexible AC transmission systems", *IEE Proceedings -Generation Transmission Distribution*, vol. 139, no. 4, pp. 323-333, 1992.
- [13] A. Nabavi-Niaki, M.R. Iravani, "Steady-state and dynamic models of unified power flow controller (UPFC) for power system studies", *IEEE Trans. on Power Systems*, vol. 11, no. 4, pp. 1937-1943, 1996
- [14] P. C. Stefanov, A. M. Stankovic, "Modeling of UPFC operation under unbalanced conditions

- with dynamic phasors”, *IEEE Trans. on Power Systems*, vol. 17, no. 2, pp. 395-403, 2002.
- [15] H.F. Wang, “Damping function of unified power flow controller”, *IEE Proceedings-Generation Transmission Distribution*, vol. 146, no. 1, pp. 81-87, 1999.
- [16] H. F. Wang, “Application of modeling UPFC into multi-machine power systems”, *IEE Proceedings- Generation Transmission Distribution*, vol. 146, no. 3, pp. 306-312, 1999.
- [17] K.R. Padiyar, A.M. Kulkarni, “Control design and simulation of unified power flow controller”, *IEEE Trans. on Power Delivery*, vol. 13, no. 4, pp. 1348-1354, 1997.
- [18] E. Uzunovic, C.A. Canizares, J. Reeve, “EMTP studies of UPFC power oscillation damping”, *Proc. of the North American Power Symposium*, pp. 405-410, 1999.
- [19] N. Mithulananthan, C. Canizares, J. Reeve, G. Rogers, “Comparison of PSS, SVC, and STATCOM for damping power system oscillations”, *IEEE Trans. on Power Systems*, vol. 18, no. 3, pp. 786-792, 2003.
- [20] R.K. Pandey, N.K. Singh, “Minimum singular value based identification of UPFC control parameters”, *Proc. of IEEE Region 10 Conference*, pp. 1-4, 2006.
- [21] A.K. Baliarsingh, S. Panda, A.K. Mohanty, C. Ardil, “UPFC supplementary controller design using real-coded genetic algorithm for damping low frequency oscillations in power systems”, *International Journal of Electrical Power and Energy Systems Engineering*, vol. 3, no.4, pp. 165-175, 2010.
- [22] M. Tripathy, S. Mishra, G.K. Venayagamoorthy, “Bacteria foraging: a new tool for simultaneous robust design of UPFC controllers”, *Proc. of the International Joint Conference on Neural Networks*, pp. 2274-2280, 2006.
- [23] Y. Lee, S. Yung, “STATCOM controller design for power system stabilization with sub-optimal control strip pole assignment”, *International Journal of Electrical Power and Energy Systems*, vol. 24, no. 9, pp. 771-779, 2002.
- [24] A. Ajami, R. Gholizadeh, “Optimal design of UPFC-based damping controller using imperialist competitive algorithm”, *Turkish Journal of Electrical Engineering and Computer Sciences*, vol. ?, no. 201(Sup.1), pp. 1109-1122, 2011.
- [25] A. Ajami, H. Asadzadeh, “Damping of Power System Oscillations Using UPFC Based Multipoint Tuning AIPSO-SA Algorithm”, *Gazi University Journal of Science*, vol. 24, no. 4, pp. 791-804, 2011.
- [26] J. Kennedy, R.C. Eberhart, “Particle swarm optimization”, *Proc. of IEEE International Conference on Neural Networks*, pp. 1942-1948, 1995.
- [27] E. Rashedi, S. Nezamabadi, S. Saryazdi, “GSA: a gravitational search algorithm”, *Information Sciences*, vol. 179, no. 13, pp. 2232-2248, 2009.
- [28] A.A. Atapour, A. Ghanizadeh, S.M. Shamsuddin, “Advances of Soft Computing Methods in Edge Detection”, *International Center for Scientific Research and Studies*, vol. 1. no. 2, pp. 162-202, 2009.
- [29] E. Rashedi, H. Nezamabadi-pour, S. Saryazdi, “BGSA: binary gravitational search algorithm”, *Natural Computing* vol. 9, no. 3, pp. 727-745, 2009.
- [30] S. Sinaie, “Solving shortest path problem using Gravitational Search Algorithm and Neural Networks”, *Universiti Teknologi Malaysia (UTM), Joho r Bahru, Malaysia*, M.Sc. Thesis 2010.
- [31] S. Mirjalili and S.Z. Mohd Hashim, “A New Hybrid PSO-GSA Algorithm for Function Optimization”, *Proc. of the International Conference on Computer and Information Application (ICCIA)*, pp. 374-377, 2010.
- [32] M.A. Abido, A.T. Al-Awami, Y.L. Abdel-Magid, “Power system stability enhancement using simultaneous design of damping controllers and internal controllers of a unified power flow controller”, *IEEE PES General Meeting*, 2006.